Dewetting at the interface between two immiscible polymers

1997 J. Phys.: Condens. Matter 9 7741

(http://iopscience.iop.org/0953-8984/9/37/007)

J. Phys.: Condens. Matter **9** (1997) 7741–7752. Printed in the UK PII: S0953-8984(97)80582-6

Dewetting at the interface between two immiscible polymers

G Krausch

Institut für Physikalische Chemie, Ludwig-Maximilians-Universität München, Theresienstrasse 39, D-80333 München, Germany

Received 2 January 1997

Abstract. We review the recent theoretical and experimental efforts that have been made in studying the dynamics of dewetting at the interface between two liquids. While detailed theoretical predictions are already available, the experimental studies are still at an early stage. The first experiments using high-molecular-weight homopolymers not only enable a study of the dewetting dynamics to be made, but also allow a detailed analysis of the deformed liquid/liquid interface around the growing holes to be undertaken. The experimental results are compared with theoretical predictions.

1. Introduction

The dewetting of thin liquid films from a flat surface is a common phenomenon, with a crucial impact on various technological processes. In recent years, the stability of thin liquid films has aroused considerable scientific interest as well, and a basic understanding of spreading and dewetting has evolved both for simple liquids and for complex fluids [1–15]. Thin polymer films with high molecular weights have proven to be ideal model systems in these studies, owing to their low vapour pressure and due to the fact that their high viscosity facilitates the study of the dynamic behaviour. Moreover, the long-chain character of the polymer molecules adds some complexity to the dynamic processes involved during dewetting, thus making the study of polymer dewetting an interesting subject in itself. Unique phenomena have recently been observed for the dewetting of polymer films: films thinner than the bulk equilibrium size of their constituent molecules were shown to dewet spontaneously [6], and dewetting was actually shown to be a suitable probe for the mobility in ultra-thin polymer films [7], in which the entanglement density may be significantly reduced due to geometric constraints. The stability of thin liquid films on solid substrates modified through the attachment of polymer chains was studied as well. Klein and co-workers observed that a low-molecular-weight liquid could be stabilized against dewetting by the use of a polymer brush [14]. Rafailovich and co-workers on the other hand were able to show that a high-molecular-weight polymer dewets a polymer brush of even the same material, due to the particular molecular architecture at the substrate (brush) surface [15].

Although some of the above-mentioned studies used polymeric or polymer-modified surfaces as substrates for the dewetting experiments, they all fall into the category of liquid films dewetting from a *solid* substrate. The notion of a solid substrate implies that the liquid/substrate interface is a non-deformable plane, and the viscous dissipation during the dewetting process takes place solely within the dewetting film. In this case the equilibrium

0953-8984/97/377741+12$19.50

contact angle is easily calculated by balancing the in-plane components of the surface and interfacial tensions. This procedure leads to the well known Young equation. In contrast, the more complex situation of a liquid dewetting from a *liquid* substrate has received much less attention [12, 16–20]. Here, the interface between the two liquids can deform to minimize the total free energy of the system, and viscous dissipation may take place in the dewetting film *and* in the substrate. Both horizontal and vertical components of the surface and interfacial tensions need to be balanced to reveal the equilibrium contact angles, and Young's equation is replaced by the von Neumann construction.

Experimentally, the situation of liquid/liquid dewetting is somewhat more demanding, since the actual shape of the liquid/liquid interface needs to be monitored during the dewetting process, in addition to the growth of the holes in the dewetting film. While the latter is easily accomplished using optical microscopy, imaging the three-dimensional buried interface between the two liquids turns out to be a rather tedious experimental task. Again, high-molecular-weight polymers turn out to be useful experimental model systems. The dewetting process is easily interrupted by cooling the sample below the glass transition, thereby effectively freezing in the structure around the growing holes for further analysis. The polymer/polymer interface can then be imaged in the glassy state via cross-sectional electron microscopy [17, 18] or via atomic force microscopy (AFM) [19, 20] (after selective dissolution of the dewetting phase). In addition, the viscosities of the substrate and dewetting layer are easily varied by variation of the respective molecular weights without significantly changing the interfacial tension between the two materials (provided that the molecular weights are high enough). The first experiments of this type have recently been reported. In contrast to the somewhat limited experimental data available at present, a quite comprehensive theoretical study of the problem was recently presented by Brochard-Wyart and co-workers [12]. Their results suggest that liquid–liquid dewetting should exhibit a variety of different regimes depending mainly on the relative viscosities of the two liquids, the thicknesses of the respective liquid layers, and the surface and interfacial tensions involved.

In the present paper, we shall review the results on liquid/liquid dewetting obtained so far for polymer systems. We exclude from our discussion the variety of dewetting experiments performed on polymer films on solid, i.e. undeformable substrates. We start by summarizing some of the relevant theoretical results. We then review some of the recent experimental studies aiming to test the theoretical predictions.

2. Theoretical considerations

As was mentioned above, most of the theoretical work on the dynamics of dewetting has concentrated on the case of a liquid film dewetting from a solid substrate. The more general case of a liquid dewetting from a liquid substrate has recently been treated by Brochard-Wyart and co-workers in quite some detail [12]. For the present discussion, we briefly summarize their results, following their notation for simplicity. The interested reader is referred to the original paper for further details. We start by noting that whether a substrate will be considered 'liquid' or 'solid' is no longer determined by the inherent properties of the substrate itself, but rather is indicated by the relative viscosities of both the substrate and the dewetting film. Therefore, almost any material may act both as a solid and a liquid substrate provided that the dewetting film has a significantly lower (higher) viscosity under the respective experimental conditions. From this perspective, the dewetting of a liquid from a solid is merely one particular scenario of liquid/liquid dewetting.

Consider the system shown in figure 1, where A and B are two liquid phases. γ_A and

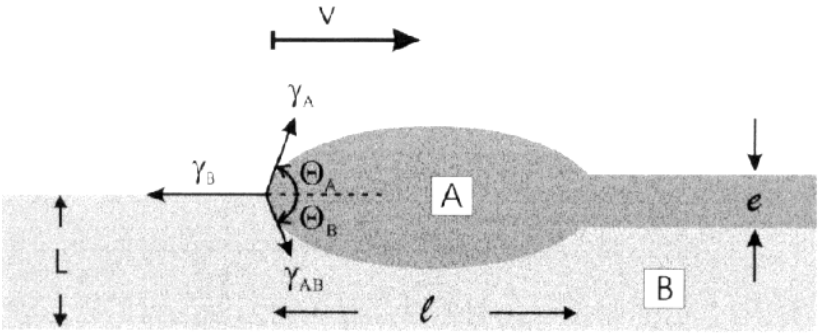

Figure 1. A schematic drawing of the situation in liquid/liquid dewetting.

γ_B are the surface tensions of A and B respectively, and γ_{AB} is the A–B interfacial energy. The wetting behaviour is described by the spreading parameter S:

$$S = \gamma_B - (\gamma_A + \gamma_{AB}). \tag{1}$$

A dewets B when $S < 0$. In contrast to the situation of a liquid dewetting a solid surface, here the AB interface is no longer constrained to be a plane, but adjusts itself to minimize the surface free energy. The macroscopic equilibrium contact angles are determined by the von Neumann construction, i.e. both horizontal and vertical components of the capillary force must vanish at the contact line. In the limit of small angles Θ_A and Θ_B, one finds

$$\gamma_A \Theta_A = \gamma_{AB} \Theta_B \tag{2}$$

and

$$-S = \frac{1}{2}(\gamma_A \Theta_A^2 + \gamma_{AB} \Theta_B^2). \tag{3}$$

With $\Theta_E = \Theta_A + \Theta_B$, and an effective surface tension $\gamma^{-1} = \gamma_A^{-1} + \gamma_{AB}^{-1}$, this leads to

$$S = -\frac{1}{2}\gamma \Theta_E^2. \tag{4}$$

The stability of a film with respect to dewetting is determined from the free energy per unit area. For macroscopic films (i.e. films thicker than a few micrometres), the free energy is given by a sum of capillary and gravitational energies, whereas for microscopically thin films, long-range van der Waals forces dominate.

So far we have only dealt with the equilibrium wetting situation. An initially homogeneous and flat-top film may dewet through the formation of holes [21]. The holes are surrounded by a rim carrying the excess material. Driven by capillary forces, the holes grow and, consequently, the rims move outward as dewetting proceeds. During this process, a dynamic contact angle Θ_D is observed, rather than the equilibrium contact angle Θ_E. When the holes have grown sufficiently large, the rims will meet, and a transient two-dimensional network of rims is formed. The rims then undergo a Rayleigh instability and break up into isolated droplets.

In the following, we shall review in some detail the results of reference [12] concerning the dynamics of hole growth after formation. As mentioned qualitatively at the beginning of this section, different regimes are expected depending on the relative viscosities η_i of the two liquids. If the viscosity of the lower layer B is significantly higher than the viscosity of the dewetting film, i.e. if $\eta_B > \eta_A/\Theta_E$, the lower layer is solid-like. In the opposite

case, i.e. for $\eta_B < \eta_A/\Theta_E$, the lower layer behaves like a liquid. We shall refer to the two scenarios as solid-substrate behaviour and liquid-substrate behaviour, respectively. For the solid-substrate case, two regimes can be distinguished: a viscous regime, where liquid A is viscous and has a small contact angle; and an inertial regime, where A has a low viscosity and a large contact angle. In the viscous regime, the growth of the hole is controlled by the competition of capillary forces and viscous flow of the A material. The radius of the growing hole is predicted to grow linearly with time. Therefore, the dewetting velocity is constant, and is given by

$$v = \frac{1}{12\,ln\sqrt{2}}\frac{\gamma_A}{\eta_A}\Theta_E^3 \tag{5}$$

with ln being a numerical factor of order 10. Note that the velocity v is independent of the viscosity of the lower layer. The scaling of the dewetting velocity with the cube of the contact angle was first predicted by Tanner. Equation (5) is valid if the width $l(t)$ of the rim is smaller than the diameter $R(t)$ of the hole, i.e. if the velocities of the inner and outer contact lines are the same. The velocities are related to the dynamic contact angle Θ_D, which in this regime is given by

$$\Theta_D = \Theta_E/\sqrt{2}. \tag{6}$$

Conservation of the volume of A leads to a relation between the width $l(t)$ of the rim and the diameter $R(t)$ of the growing hole:

$$l(t) \propto \sqrt{R/\Theta_E}. \tag{7}$$

Thus, since R increases linearly with time in the regime of constant dewetting velocity, $l(t) \sim t^{1/2}$.

If the dewetting liquid has a very low viscosity, viscous dissipation becomes negligible (the 'inertial regime'). Here, the driving force on the rim is simply $-S$, and the velocity of the rim is given by

$$v = \sqrt{\frac{|S|}{\rho_A e}}. \tag{8}$$

ρ_A and e are the density and the thickness of the top layer, respectively. The finding of a constant velocity (although the rim is driven by a constant force) is due to the fact that the mass of material in the rim is continuously increasing as the hole grows.

For the case of a highly viscous liquid dewetting from a low-viscosity substrate, $\eta_B < \eta_A/\Theta_E$, viscous dissipation is dominated by the contribution of the substrate. Three regimes are distinguished depending on the viscosity of the substrate: a viscous regime similar to the one discussed, a visco-inertial regime, and a purely inertial regime. In the viscous regime, a constant dewetting velocity is predicted provided that the thickness of the substrate is larger than the lateral size of the rim (the 'bulk substrate'):

$$v = \left(\frac{\gamma}{\eta_B}\right)\Theta_E^2. \tag{9}$$

In contrast to the situation described above, however, v now depends on the substrate viscosity η_B rather than on η_A. The situation changes significantly when the thickness of the substrate becomes comparable to or smaller than the rim size $l(t)$. In this case, the radius $R(t)$ of the holes is no longer expected to increase linearly with time, and the velocity becomes time dependent:

$$v \propto \left(\frac{\gamma_B^2 L^2 \Theta_e}{\eta_B^2 e}\right)^{1/3} t^{-1/3}. \tag{10}$$

L and e are the thicknesses of the B and A layers respectively.

For smaller substrate viscosity, one enters a regime where the flows induced in the substrate by the moving rim cannot follow adiabatically. A crossover from the viscous into this visco-inertial regime is expected for $l = l_c = \eta_B^2/\rho_B S$. For a rim larger than l_c, the penetration length of the flow into the lower layer induced by the motion of the rim is smaller than the rim size. The flows in the substrate are confined to a diffusion layer of thickness $d = (\eta_B/\rho_B)^{1/2} t_b^{1/2}$, with t_b being the rim passage time $t_b = l/v$. The sizes of the holes are predicted to follow a power law, with an exponent close to but smaller than unity:

$$R(t) = \frac{S^{4/3}\Theta_E^{1/7}}{e^{1/7}\eta_B^{2/7}\rho_B^{2/7}} t^{6/7}. \tag{11}$$

Finally, for very small substrate viscosities, an inertial regime is expected as discussed above for the case of low-viscosity top layers.

3. Experimental observations

The first experimental study on liquid/liquid dewetting was reported by Martin *et al* [16], who investigated metastable poly(dimethylsiloxane) (PDMS) films deposited onto a substrate of poly(fluoroalkylmethylsiloxane) (PFAS). The viscosity of the liquid substrate was varied by changing the molecular weight. The relative viscosities studied ranged over $1 < \eta_{\mathrm{PDMS}}/\eta_{\mathrm{PFAS}} < 50$, and all fell into the liquid-substrate regime. Macroscopically thick PFAS films were contained in a Petri dish, and films of PDMS were deposited to the liquid substrate by solvent evaporation from isopentane. Holes were nucleated in the PDMS film via an external perturbation, and the growth of the holes was followed by optical microscopy.

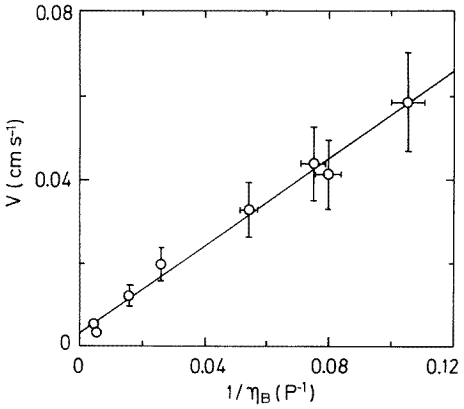

Figure 2. The dewetting velocity as a function of the substrate viscosity for PDMS film deposited onto PFAS substrate layers. The thickness of the PDMS film was 100 mm. (From reference [16].)

In agreement with the prediction of equation (9), a linear growth law was observed for all PFAS viscosities studied. The velocity was found to scale inversely with the underlayer viscosity. This is shown in figure 2. A variation of the PDMS viscosity did not significantly affect the result. This finding is also in agreement with the prediction for the liquid-substrate regime. The authors observed a strong decrease of the dewetting velocity with increasing

PDMS film thickness between 50 μm and 1 mm. For such thick films, the energy is dissipated in a rather large volume. The friction coefficient now becomes dependent on the ratio between the thickness of the liquid underlayer and the rim width. As gravity flattens the rim, the friction coefficient becomes dependent on the upper-layer thickness. In addition, due to hydrostatic pressure induced by gravity, an additional (gravity-related) contribution to the spreading parameter needs to be considered. After suitable modification of equation (9), the authors were able to obtain good agreement between the experimental data and the theoretical prediction.

While the above results are in good agreement with the theoretical predictions, an experimental test of the assumed morphology of the rim around the growing hole was not carried out. The first experiments of this type were reported by Faldi *et al* [17], who used a variety of techniques in trying to establish the exact shape of the rim. The authors studied the dewetting of polycarbonate (PC) films 200 nm thick on substrate films of poly(styrene-co-acrylonitrile) (SAN) 200 nm thick, supported on a rigid substrate. In contrast to the case for the experiments made by Martin *et al* [16], the films were thin enough to undergo spontaneous dewetting. The dewetting process was studied at 190 °C. To investigate the morphology of the films, the dewetting process was deliberately interrupted by quenching the films below the glass transition temperature. Atomic force microscopy (AFM), Auger electron spectroscopy (AES), and cross-sectional secondary-electron microscopy (SEM) were used to study the surface morphology, the surface chemical composition, and the interface deformation around the growing holes, respectively. In a later study, the authors also investigated the dynamics of dewetting as a function of the SAN composition [18].

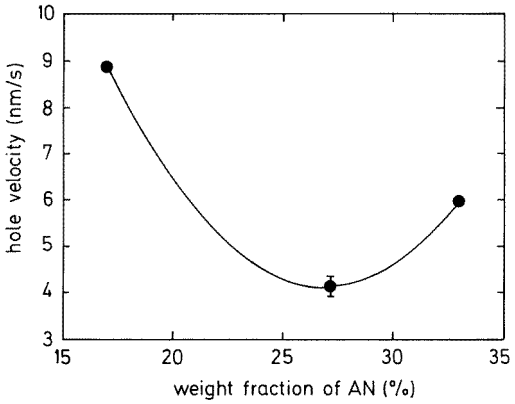

Figure 3. The dewetting velocity as a function of the AN content in PS/SAN bilayers. The solid line is a guide to the eye. (From reference [18].)

We start with the morphology of the film in the vicinity of the growing holes. The cross-sectional SEM experiments showed that, in contrast to the assumption of the theoretical model, the profile of the rim was not semicircular, but was asymmetric. The rim was found to be much steeper towards the inside of the holes than towards the continuous PC film outside the holes. In addition, the deformation of the polymer/polymer interface was found to be much less developed than the deformation of the PC/air interface. AES measurements inside and outside the holes showed that the PC layer was completely removed inside the hole. AFM measurements indicated that the dewetting PC film pulled some SAN into the rims, thereby reducing the SAN film thickness inside the holes. The central result of this work is certainly the finding that the particular morphology around the growing holes may

deviate considerably from the simple notion depicted in figure 1. The same authors also studied the dynamics of hole growth in the same system for varying AN content in the SAN substrate layer. Again, a constant dewetting velocity was observed. The velocity was found to exhibit a minimum for AN weight fractions around 25–30% (figure 3). With changing AN content, the χ-parameter of the PC/SAN system, and thereby the interfacial tension between the two polymers, is changed. With χ being minimal around about the same SAN weight fraction, the interfacial tension, and thereby the contact angle, should be minimal. Consequently, the dewetting velocity should exhibit a minimum, as observed.

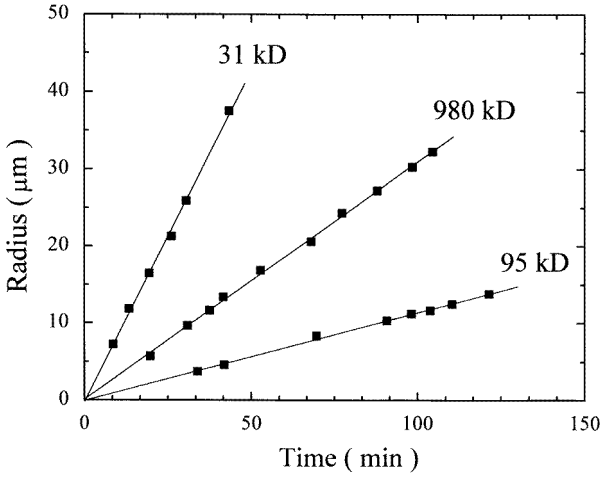

Figure 4. Radii of holes in the PS layer as a function of time t for various molecular weights of the PMMA substrates ($M_{w,PS} = 95$ kilodaltons, $T = 170$ °C). (From reference [19].)

At around the same time, Lambooy *et al* have studied the dewetting behaviour of thin polystyrene (PS) films from poly(methylmethacrylate) (PMMA) substrates [19]. They combined measurements of the dewetting dynamics (for varying relative viscosities of the two polymers) with the determination of the rim morphology around the growing holes. The substrate films were spun cast onto silicon wafers. The PS films were first spun onto glass slides, floated onto deionized water, and picked up onto the PMMA substrate layers. At around 160 °C, $S_{PS/PMMA} < 0$, so PS tends to dewet PMMA. The viscosity of the layers was varied over a wide range by using monodisperse batches of different molecular weights. Well characterized samples with narrow molecular weight distributions are readily available for both materials. In the range of molecular weights studied, the surface and interfacial energies of the two materials do not significantly change with changing chain length. Therefore, the viscosities of the two liquids can be varied in a controlled way, with all other relevant parameters being fixed. The authors followed the growth of the holes *in situ* using optical microscopy. To establish the shape of the PS/PMMA interface in the vicinity of the growing hole, samples were quenched below the glass transition at various times during the dewetting process. Then, the free surface of the film was imaged with AFM. Subsequently, the PS top layer was selectively removed by immersing the samples into cyclohexane. After drying, the same spot on the sample was located again, and the remaining PMMA surface (i.e. the former PS/PMMA interface) was imaged with AFM. Superposition of the two AFM images then provided three-dimensional images of the PS rim around a growing hole. In contrast to the use of cross-sectional SEM, this procedure

allows one to image an entire hole, rather than an arbitrary cross-section. For quantitative analysis, cross-sections of the AFM images at well defined locations (generally through the centres of the holes) are easily produced during numerical data processing after the experiment.

In their study, Lambooy *et al* concentrated on the influence of the substrate layer viscosity on the dewetting velocity. Figure 4 shows the growth of the holes in a PS layer 124 nm thick ($M_{w,PS} = 95$ kilodaltons) on top of PMMA layers 95 nm thick, of varying molecular weight. Snapshots of the growing holes were taken with optical microscopy, and the radii were extracted from the digitized images by a straightforward numerical analysis. The first snapshots were taken as soon as the holes had grown large enough to be resolved by optical microscopy (a few microns). The experiment was stopped before the holes started to coalesce. Within this time window, a linear growth behaviour was found in all cases, indicating a constant dewetting velocity v. Figure 5 shows the dewetting velocity plotted as a function of the PMMA viscosity for two different PS molecular weights. For low PMMA molecular weights, the dewetting velocity was found to decrease with increasing PMMA viscosity, in agreement with the results discussed above. However, with increasing PMMA molecular weight, the dewetting velocity exhibits a minimum, and then starts increasing again. This behaviour was found for all of the PS molecular weights studied, with the location of the minimum being shifted to higher PMMA molecular weights with increasing PS molecular weight.

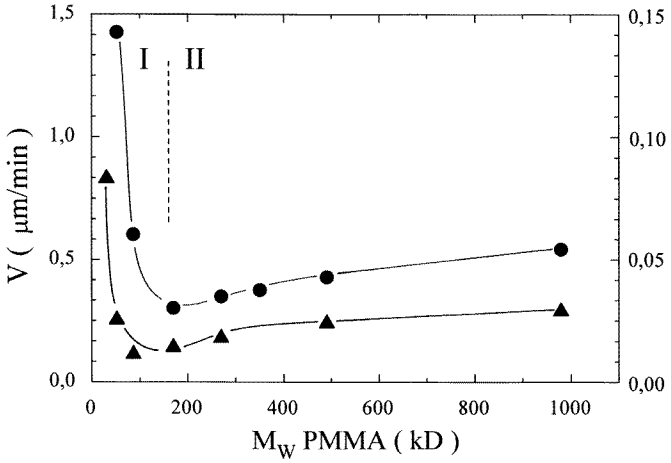

Figure 5. The dewetting velocity $v = \mathrm{d}R/\mathrm{d}t$ of thin PS films from a thin PMMA underlayer, as a function of the molecular weight of the PMMA. Triangles: $M_{w,PS} = 95$ kilodaltons, $T = 170\ ^{\circ}$C (left-hand scale); circles: $M_{w,PS} = 177$ kilodaltons, $T = 180\ ^{\circ}$C (right-hand scale). The solid lines are guides to the eye. (From reference [19].)

The non-monotonic behaviour of the dewetting velocity observed in figure 5 suggests that the relative viscosities investigated in this study span both the liquid-substrate regime (low PMMA molecular weights) and the solid-substrate regime (high PMMA molecular weights) as discussed in section 2. To verify a transition between the two regimes experimentally, the authors have imaged the PS-PMMA interfaces around the growing holes for different molecular weight combinations. As an example, figure 6 shows part of the edge of a hole before and after selective removal of the PS top layer for the low-PMMA-molecular-weight case ($M_{w,PS} = 95$ kilodaltons, $M_{w,PMMA} = 31$ kilodaltons). In figure

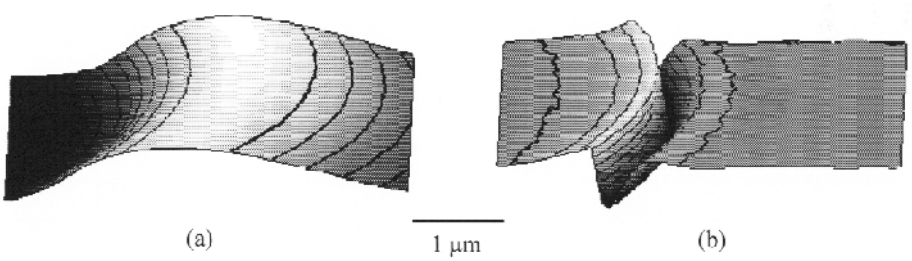

Figure 6. AFM images of the right-hand edge of a 25 μm wide hole before (a) and after (b) removal of the PS top layer using a selective solvent ($M_{w,PS} = 95$ kilodaltons, $M_{w,PMMA} = 31$ kilodaltons; $T = 180\ ^{\circ}$C). Black contour lines are included for clarity. These lines connect points of equal height; since raw data are shown without any smoothing, the lines appear somewhat fuzzy in areas of small surface slope. (From reference [19].)

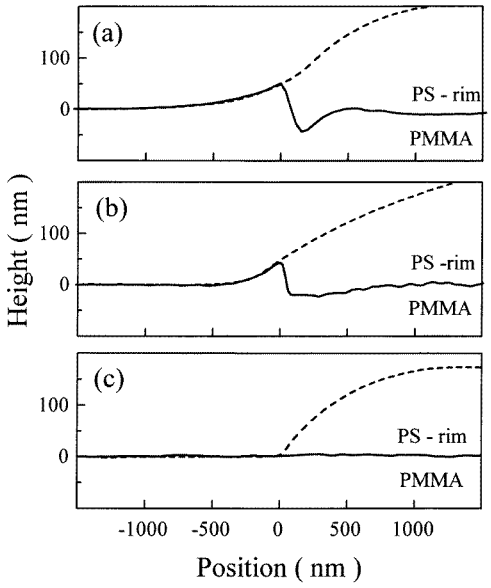

Figure 7. Cross sections through AFM images taken at the same holes before (dashed line) and after (solid line) removal of the PS top layer for different PMMA molecular weights. ($M_{w,PS} = 95$ kilodaltons; $M_{w,PMMA} = 31$ kilodaltons, 126 kilodaltons, and 491 kilodaltons.)

6(b), the curved shape of the bottom part of the rim clearly shows that the PS rim extends considerably into the PMMA substrate layer, thereby confirming the notion of a deformable interface between the two materials. We also note that the AFM images indicate that the interface deformation is highly localized near the contact line, and extends far less than the apparent width of the rim as determined from the deformation of the free PS surface. We shall return to this issue below. In figure 7, cross-sections of such AFM images are shown for varying PMMA molecular weight. The dashed lines correspond to images taken before PS removal, whereas the solid lines correspond to images taken at the same spot after immersing the samples in cyclohexane. It becomes clear from figure 7 that with increasing PMMA molecular weight, a transition from a liquid-like substrate (a deformable interface) to a solid-like substrate (a flat interface) occurs. Qualitatively, the dewetting

velocity v depends strongly on the PMMA molecular weight for low PMMA viscosity, in agreement with the theoretical prediction. With increasing PMMA viscosity the amount of interface deformation, and thereby the contribution of viscous dissipation within the PMMA substrate, becomes smaller. Eventually, the dewetting velocity should become independent of the PMMA molecular weight (the solid-substrate regime), and reach a limiting value depending on the PS viscosity. This trend is at least qualitatively reproduced by the data shown in figure 7.

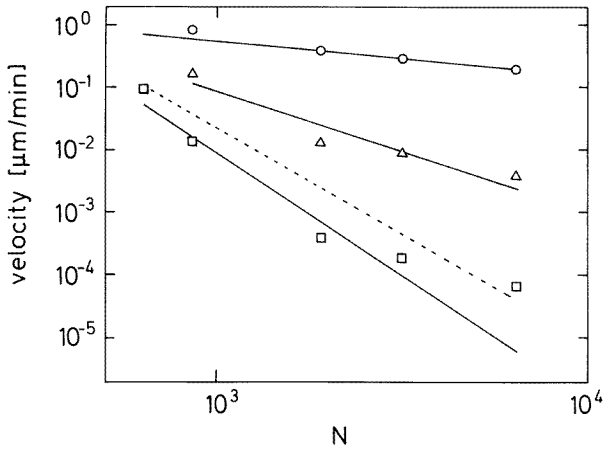

Figure 8. A double-logarithmic presentation of the dewetting velocity as a function of the PS molecular weight. The PMMA molecular weight was 27 kilodaltons (circles), 88 kilodaltons (triangles), and 330 kilodaltons (squares). The 330 kilodaltons data have been shifted vertically. The solid lines are linear least-squares fits. The dashed line indicates the theoretical prediction according to equation (5). (From reference [20].)

While the study made by Lambooy *et al* remained rather qualitative, a more quantitative study of the same system was recently reported by Qu *et al* [20]. The authors investigated a wider range of molecular weights, and tried to establish the scaling behaviour of the dewetting velocity as a function of the PS molecular weight for different PMMA substrates. Again, optical microscopy and atomic force microscopy are used to monitor the hole growth and determine the interfacial shape. Following Brochard-Wyart's predictions, one would expect the dewetting velocity to be independent of the PS molecular weight for low PMMA viscosities, and scale inversely proportionally with the PS viscosity for sufficiently high PMMA molecular weights. Given that the PS molecular weights are high enough that the molecular motion is governed by reptation, the dewetting velocity is expected to scale with the PS molecular weight as $N_{\mathrm{PS}}^{-3.4}$ in this regime. Figure 8 shows the results obtained by Qu *et al* in a double-logarithmic presentation. The solid lines are least-squares fits to the data. For the lowest PMMA molecular weight ($M_{\mathrm{w,PMMA}} = 27$ kilodaltons), the dewetting velocity is indeed only slightly varying with the PS molecular weight. For the highest PMMA molecular weight ($M_{\mathrm{w,PMMA}} = 330$ kilodaltons), the velocity is found to scale with the PS molecular weight as $N_{\mathrm{PS}}^{-3.9\pm0.6}$. Within the experimental error, the exponent agrees with the predicted value for the solid-substrate regime. For the intermediate PMMA molecular weight, a smaller exponent is found. The results agree well with the theoretical predictions outlined in section 2.

So far, the experimental results obtained by Lambooy *et al* and Qu *et al* have indicated a constant dewetting velocity, irrespective of the viscosities of the two materials. Given that

in both cases the thickness of the PMMA layers ranged around 100 nm, while the widths of the rims measured a few microns, this finding is somewhat at variance with the prediction of a thin-substrate regime for liquid substrates (equation (9)). As discussed above, the holes are expected to follow a $t^{2/3}$-growth law once the thickness L of the liquid substrate becomes smaller than the size l of the rim. Although the AFM images of the PS/PMMA interface show that the interface deformation is localized close to the contact line, it is still larger than the thickness of the PMMA layer. Here, further experimental work will be needed. The experiments made by Qu *et al* gave some first indications for non-linear hole growth at the lowest PMMA molecular weight; however, the data did not allow us to unambiguously establish a growth exponent. The first unpublished results obtained by Phelan *et al* [22] show that the growth exponent changes as the PMMA film thickness becomes significantly smaller than 100 nm. Their results indicate a strong decrease in the dewetting velocity (by almost an order of magnitude) once the PMMA film thickness becomes as small as 10 nm. For such thin films, the mobility of the PMMA chains may be significantly reduced due to adsorption at the silicon substrate. Here, dewetting experiments may well prove to be suitable probes for investigating the polymer mobility in the presence of a surface and in ultra-thin films.

4. Conclusion

We have reviewed the recent theoretical and experimental efforts that have been made in an effort to achieve an understanding of the dynamics of liquid/liquid dewetting. It turns out that the particular properties of long-chain molecules make them ideal experimental model systems, strongly facilitating the experimental study of both the dynamics of hole growth and the morphology of the hole/rim system during the process of dewetting. The three-dimensional imaging of the buried interface between the two liquids at any stage of the rupture process allows critical testing of the theoretical model calculations. The general dependence of the dewetting velocity as a function of the relative viscosities of the two liquids could be verified both for the liquid- and solid-substrate cases. However, quite a few questions remain open. To name just a few areas, the exact shapes of the rim and the liquid/liquid interface, as well as the shape of the underlayer/vacuum interface within the growing holes, seem to be more complex than was initially assumed in the theoretical studies, and they need further consideration. The influence of the supporting solid substrate on the dewetting dynamics for the case of ultra-thin liquid underlayers needs to be established, and the predicted transition between a bulk substrate and a thin substrate remains to be observed experimentally. In addition, the late stage of dewetting, i.e. the rupture of the rim network and the formation and shape of droplets, has hardly been looked at. In view of the various experimental efforts that are under way at present, quite a few new insights are to be expected in the near future.

Acknowledgments

Generous financial support through the Deutsche Forschungsgemeinschaft and through the Stiftung Volkswagenwerk is gratefully acknowledged. The author benefited from helpful discussions with M H Rafailovich.

References

[1] Cazabat A-M 1987 *Contemp. Phys.* **28** 347
[2] de Gennes P G 1985 *Rev. Mod. Phys.* **57** 827
[3] Silberzahn P and Leger L 1992 *Macromolecules* **25** 1267
Silberzahn P and Leger L 1991 *Phys. Rev. Lett.* **66** 185
[4] Redon C, Brochard-Wyart F and Rondelez F 1991 *Phys. Rev. Lett.* **66** 715
[5] Reiter G 1992 *Phys. Rev. Lett.* **68** 75
[6] Zhao W, Rafailovich M H, Sokolov J, Fetters L J, Plano R, Sanyal M K, Sinha S K and Sauer B B 1993 *Phys. Rev. Lett.* **70** 1453
[7] Reiter G 1993 *Langmuir* **9** 1344
[8] Redon C, Broszka J B and Brochard-Wyart F 1994 *Macromolecules* **27** 468
[9] Reiter G 1994 *Macromolecules* **27** 3046
[10] Brochard-Wyart F and Daillant J 1990 *Can. J. Phys.* **68** 1084
[11] Brochard-Wyart F, Redon C and Sykes C 1992 *C. R. Acad. Sci., Paris* II **314** 19
[12] Brochard-Wyart F, Martin P and Redon C 1993 *Langmuir* **9** 3682
[13] Shull K R and Karis T E 1994 *Langmuir* **10** 334
[14] Yerushalmi-Rozen R, Klein J and Fetters L J 1994 *Science* **263** 793
[15] To establish a polymer brush surface, the authors used a diblock copolymer with one block adsorbing preferentially to a solid substrate.
Liu Y, Rafailovich M H, Sokolov J, Schwarz S A, Zhong X, Eisenberg A, Kramer E J, Sauer B B and Satija S 1994 *Phys. Rev. Lett.* **73** 440
[16] Martin P, Buguin A and Brochard-Wyart F 1994 *Europhys. Lett.* **28** 421
[17] Faldi A, Winey K I and Composto R J 1995 *Materials Research Society Symposium Proceedings* vol 366 (Pittsburgh, PA: Materials Science Society) p 71ff
[18] Faldi A, Composto R J and Winey K I 1995 *Langmuir* **11** 4855
[19] Lambooy P, Phelan K C, Haugg O and Krausch G 1996 *Phys. Rev. Lett.* **76** 1110
[20] Qu S, Clarke C J, Liu Y, Rafailovich M H, Sokolov J, Phelan K C and Krausch G 1997 *Macromolecules* at press
[21] The holes may be formed by heterogeneous nucleation. Alternatively, it has been suggested that holes are formed by the spontaneous amplification of capillary waves (see, e.g., reference [12]). In the experiments discussed in the present paper, the question of hole formation has not been addressed. As a matter of fact, for the late-stage dynamics of dewetting, the original mechanism of hole formation should be irrelevant, so we shall not pursue this issue any further in the present paper.
[22] Phelan K C, Rafailovich M H, Sokolov J and Krausch G 1997 in preparation